Chapter 14

LANDAU DAMPING

As we have seen in previous chapters, collective instabilities occur in bunched and unbunched beam as a result of the interaction of the beam particles with their own wake fields. There are various way to damp these instabilities. Aside from mechanical dampers, there is a natural stabilization mechanism against collective instabilities when the beam particles have a small spread in their frequencies, such as betatron frequency, synchrotron frequency, or revolution frequency as the situation requires. This damping mechanism is called Landau damping, which was first formulated by Landau [1]. However, that paper is rather difficult to understand. Later, Jackson [2] wrote an article on longitudinal plasma oscillations and had the concept well explained.

Neil and Sessler [3] first formulated the theory of Landau damping on longitudinal instabilities, while Laslett, Neil and Sessler [4] first applied the theory to transverse instabilities. There have been quite a number of good papers written on this subject by Hereward [5], Hofmann [6], and Chao [7].

We encountered Landau damping in Chapter 5 when we formulated the dispersion relation using the Vlasov equation. There, we came across the ambiguity of a singularity in the denominator which is critical in determining whether the system will be stable or unstable. That ambiguity can only be avoided when the problem is treated as an initial-value problem. This will be covered in this chapter. We first study the beam response of an harmonic driving force, the beam response of shock or δ-pulse excitation, and finally try to understand the physics of Landau damping.

14.1 HARMONIC BEAM RESPONSE

A particle having a natural angular frequency ω is driven by a force of angular frequency Ω. The equation describing its displacement $x(t)$ is

$$\ddot{x} + \omega^2 x = A\cos\Omega t \ , \tag{14.1}$$

where A denotes the amplitude of the force or its effect on acceleration. The most general solution is

$$x(t) = x_0\cos\omega t + \dot{x}_0\,\frac{\sin\omega t}{\omega} + \frac{A}{\omega^2-\Omega^2}\left[\cos\Omega t - \cos\omega t\right] \ , \tag{14.2}$$

where x_0 and $\dot{x}_0$ are, respectively the initial value of x and $\dot{x}$ at $t=0$. The first two terms are due to a shock of δ-pulse excitation. Although they are important, we shall postpone the discussion to the next section.

Let us pay attention to the excitation by the harmonic force. Notice that the response is well-behaved even at $\omega=\Omega$. For a large number of particles having a distribution $\rho(\omega)$ in frequency and normalized to unity, the displacement of the center of mass is

$$\langle x(t)\rangle = \int_{-\infty}^{\infty} d\omega\,\frac{\rho(\omega)}{\omega^2-\Omega^2}\left[\cos\Omega t - \cos\omega t\right] \ . \tag{14.3}$$

As is the case in particle beams, the distribution is mostly a narrow one centered at angular frequency ω_x. For simplicity, let us assume that this distribution does not peak at any other frequency, even the negative frequencies. In order to drive this system of particles, the driving frequency must also be close to this center frequency, or $\Omega\approx\omega_x$. We can therefore do the expansion $\omega=\Omega+(\omega-\Omega)$, and the Eq. (14.3) can be approximated by

$$\langle x(t)\rangle = \frac{A}{2\omega_x}\left[\cos\Omega t\int_{-\infty}^{\infty} d\omega\rho(\omega)\frac{1-\cos(\omega-\Omega)t}{\omega-\Omega} + \sin\Omega t\int_{-\infty}^{\infty} d\omega\rho(\omega)\frac{\sin(\omega-\Omega)t}{\omega-\Omega}\right] \ . \tag{14.4}$$

Notice that we have separated the fast-oscillating term of angular frequency Ω and the slow-oscillating envelope-like terms with angular frequency $\omega-\Omega$. Also we see a part, the $\cos\Omega t$ term, that is not driven in phase* by the force, and the other part, the $\sin\Omega t$ term, that is driven in phase by the force. More discussion will follow later. The functions

$$p(\omega) = \frac{1-\cos\omega t}{\omega} \qquad \text{and} \qquad d(\omega) = \frac{\sin\omega t}{\omega} \tag{14.5}$$

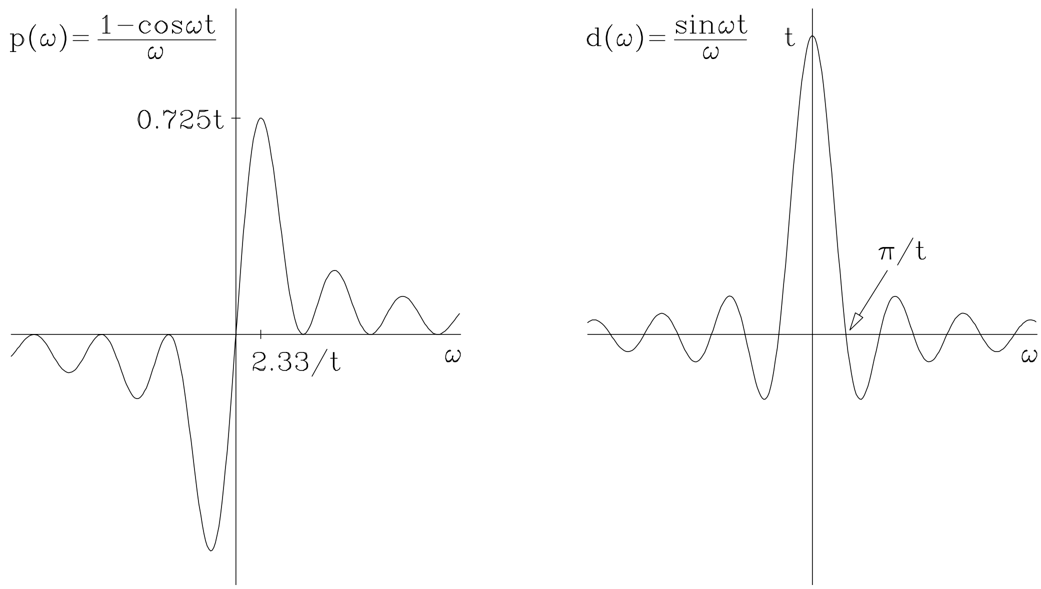

Figure 14.1: Plots of the functions $p(\omega)$ and $d(\omega)$ with t being a parameter. As $t \to \infty$, $p(\omega) \to \wp\,\omega^{-1}$ and $d(\omega) \to \pi\delta(\omega)$, where $\wp$ denotes principal value.

are illustrated in Fig. 14.1. The function $p(\omega)$ always vanishes at $\omega = 0$ and decays as ω^{-1} when $\omega \to \pm\infty$. It has peaks of value $\pm at$ at $\pm b/t$, where $b = 2.3311$ is the root of $b = \tan(b/2)$ and $a = 2b/(1+b^2) = 0.7246$. These peaks grow linearly with t and move closer to $\omega = 0$ as t increases. We therefore have

$$\lim_{t\to\infty} p(\omega) = \wp\,\frac{1}{\omega}\ , \tag{14.6}$$

where $\wp$ stands for the principal value. On the other hand, $d(\omega)$ has a peak of value t at $\omega = 0$ and rolls off as ω^{-1} for large ω, having the first zeroes at $\omega = \pm\pi/t$. As $t \to \infty$, the peak at $\omega = 0$ grows linearly while its width also shrinks inversely with t; the area enclosed is always π. Outside the peak, the function oscillates very fast. We therefore have

$$\lim_{t\to\infty} d(\omega) = \pi\delta(\omega)\ . \tag{14.7}$$

Coming back to Eq. (14.4), as $t \gg 1/\Delta\omega$, where $\Delta\omega$ is a measure of the width of the frequency distribution $\rho(\omega)$, all the transients die, leaving us with

$$\langle x(t)\rangle = \frac{A}{2\omega_x}\left[\cos\Omega t\,\wp\int_{-\infty}^{\infty} d\omega\frac{\rho(\omega)}{\omega-\Omega} + i\pi\rho(\Omega)\sin\Omega t\right]\ . \tag{14.8}$$

*Actually, "in phase" here implies the driving phase is in phase with the velocity $\dot{x}$.

Now let us repeat the derivation with the force $A\sin\Omega t$ and combine the solution with the former to get the long-term response to the force $Ae^{-i\Omega t}$:

$$\langle x(t)\rangle = \frac{Ae^{-i\Omega t}}{2\omega_x}\left[\wp\int_{-\infty}^{\infty} d\omega\,\frac{\rho(\omega)}{\omega-\Omega} + i\pi\rho(\Omega)\right] = \frac{Ae^{-i\Omega t}}{2\omega_x\Delta\omega}R(u)\ , \tag{14.9}$$

where the beam transfer function (BTF) is defined as

$$R(u) = f(u) + ig(u)\ , \tag{14.10}$$

with

$$u = \frac{\omega_x - \Omega}{\Delta\omega}\ , \tag{14.11}$$

and

$$f(u) = \Delta\omega\,\wp\int_{-\infty}^{\infty} d\omega\,\frac{\rho(\omega)}{\omega-\Omega} \qquad \text{and} \qquad g(u) = \pi\Delta\omega\rho(\omega_x - u\Delta\omega)\ , \tag{14.12}$$

where again $\Delta\omega$ is a measure of the width of the frequency distribution. The BTF is an important function, because it can be measured and it gives valuable information to the distribution function $\rho(\omega)$ and, as will be demonstrated below, also the impedance of the vacuum chamber. We can also combine the two expressions in Eq. (14.12) into one and obtain

$$R(u) = f(u) + ig(u) = \Delta\omega\int_{-\infty}^{\infty} d\omega\,\frac{\rho(\omega)}{\omega-\Omega-i\epsilon} \qquad \text{with} \qquad u = \frac{\omega_x-\Omega}{\Delta\omega}\ . \tag{14.13}$$

There can be singularity in $R(u)$ when $\Omega = \omega - i\epsilon$ or $u\Delta\omega = \omega_x - \omega + i\epsilon$. This implies that $R(u)$ is an analytic function with singularities only in the upper u-plane. Notice that instead of the derivation from the initial condition, the displacement of the center of the bunch, Eq. (14.9), can also be obtained directly by writing the force as

$$Ae^{-i(\Omega+i\epsilon)t} = Ae^{-i\Omega t}e^{\epsilon t}\ , \tag{14.14}$$

where ϵ is an infinitesimal positive number, so that the solution becomes

$$\langle x(t)\rangle = \frac{Ae^{-i\Omega t}}{2\omega_x}\int_{-\infty}^{\infty} d\omega\frac{\rho(\omega)}{\omega-\Omega-i\epsilon} = \frac{Ae^{-i\Omega t}}{2\omega_x}\left[\wp\int_{-\infty}^{\infty} d\omega\frac{\rho(\omega)}{\omega-\Omega} + i\pi\rho(\Omega)\right]\ , \tag{14.15}$$

which is exactly the same as Eq. (14.9). The addition of the small ϵ implies that the force in Eq. (14.14) is zero at $t = -\infty$ and increases adiabatically.

14.2 SHOCK RESPONSE

The beam is suddenly excited by a shock or a δ-pulse, imparting to the beam particles either a displacement x_0 or a velocity displacement $\dot{x}_0$, but not both. From Eq. (14.2), we have the shock response defined by either

$$G(t) = \frac{\langle x(t) \rangle}{x_0} = H(t) \int_{-\infty}^{\infty} d\omega\, \rho(\omega) \cos \omega t \ , \tag{14.16}$$

or

$$G(t) = \frac{\langle \dot{x}(t) \rangle}{\dot{x}_0} = H(t) \int_{-\infty}^{\infty} d\omega\, \rho(\omega) \cos \omega t \ . \tag{14.17}$$

Thus the shock response function (SRF) is always real and vanishes when $t < 0$. The SRF is important because it is an easily measured function and it can give information about the distribution function of the frequency as well as the BTF.

It is interesting to show that there is a relation between the the SRF and the BTF. The Fourier transform of the SRF is

$$\tilde{G}(\omega) = \frac{1}{2\pi} \int_{0}^{\infty} dt\, G(t) e^{i\omega t} \ . \tag{14.18}$$

where attention has to be paid that the integral starts from zero. The real part is

$$\begin{aligned} \mathcal{R}e\, \tilde{G}(\omega) &= \frac{1}{2\pi} \int_{0}^{\infty} dt\, G(t) \cos \omega t \\ &= \frac{1}{2\pi} \int_{0}^{\infty} dt\ \cos \omega t \int_{-\infty}^{\infty} d\omega'\, \rho(\omega') \cos \omega' t \\ &= \frac{1}{4\pi} \int_{-\infty}^{\infty} d\omega' \rho(\omega') \int_{-\infty}^{\infty} dt\ \cos \omega t \cos \omega' t \\ &= \frac{1}{4} \int_{-\infty}^{\infty} d\omega' \rho(\omega') \Big[\delta(\omega' - \omega) + \delta(\omega' + \omega) \Big] \\ &= \frac{1}{4} \rho(\omega) \ , \end{aligned} \tag{14.19}$$

where $\delta(\omega' + \omega)$ has no contribution because the distribution is narrow and is centered at only one positive frequency. The imaginary part is

$$
\begin{aligned}
\mathcal{I}m\,\tilde{G}(\omega) &= \frac{1}{2\pi}\int_0^\infty dt\, G(t)\sin\omega t \\
&= \frac{1}{2\pi}\int_0^\infty dt\ \sin\omega t\int_{-\infty}^\infty d\omega'\,\rho(\omega')\cos\omega' t \\
&= \frac{1}{4\pi}\int_{-\infty}^\infty d\omega'\rho(\omega')\int_0^\infty dt\left[\sin(\omega-\omega')t+\sin(\omega+\omega')t\right] \\
&= \frac{1}{4\pi}\left[\wp\int_{-\infty}^\infty d\omega'\frac{\rho(\omega')}{\omega-\omega'}+\wp\int_{-\infty}^\infty d\omega'\frac{\rho(\omega')}{\omega+\omega'}\right] \qquad (14.20)
\end{aligned}
$$

where again the last principal value integral involving $\omega+\omega'$ can be neglected because of the narrow spread of the distribution ρ. We write these integrals as principal value integrals because during the derivation, one integrand vanishes when $\omega'-\omega=0$ and the other vanishes when $\omega+\omega'=0$. Combining the result,

$$
\begin{aligned}
\tilde{G}(\omega) &= \frac{-i}{4\pi}\left[\wp\int_{-\infty}^\infty d\omega'\frac{\rho(\omega')}{\omega'-\omega}+i\pi\rho(\omega)\right] \\
&= \frac{-i}{4\pi\Delta\omega}\left[f(u)+ig(u)\right]=\frac{-i}{4\pi\Delta\omega}R(u)\ . \qquad (14.21)
\end{aligned}
$$

In other words, the Fourier transform of the SRF is equal to the BTF multiplied by $-i/(4\pi\Delta\omega)$. This also provides us with a way to compute the BTF. The procedure is: compute the SRF $G(t)$, find its Fourier transform $\tilde{G}(\omega)$, and then infer the BTF $R(u)$.

As an example, take the Lorentz distribution

$$
\rho(\omega)=\frac{\Delta\omega}{\pi}\frac{1}{(\omega-\omega_x)^2+(\Delta\omega)^2}. \qquad (14.22)
$$

The SRF is

$$
\begin{aligned}
G(t) &= H(t)\,\mathcal{R}e\int_{-\infty}^\infty d\omega\,\frac{\Delta\omega}{\pi}\frac{e^{i\omega t}}{(\omega-\omega_x)^2+(\Delta\omega)^2} \\
&= H(t)\,\mathcal{R}e\,e^{i(\omega_x+i\Delta\omega)t}=H(t)e^{-\Delta\omega t}\cos\omega_x t\ . \qquad (14.23)
\end{aligned}
$$

Next the Fourier transform,

$$\begin{aligned}\tilde{G}(\omega) &= \frac{1}{2\pi}\int_0^\infty dt\ \cos\omega_x t\, e^{(-\Delta\omega+i\omega)t} \\ &= \frac{1}{4\pi}\int_0^\infty dt\ \left[e^{i(\omega_x+i\Delta\omega+\omega)t}+e^{i(-\omega_x+i\Delta\omega+\omega)t}\right] \\ &= \frac{1}{4\pi}\left[\frac{1}{-i(\omega_x+\omega+i\Delta\omega)}+\frac{1}{i(\omega_x-\omega-i\Delta\omega)}\right] \\ &= \frac{-i}{4\pi\Delta\omega}\,\frac{1}{u-i} = \frac{-i}{4\pi\Delta\omega}\,\frac{u+i}{u^2+1}\ ,\end{aligned} \tag{14.24}$$

where again the smaller term involving $\omega_r+\omega$ has been removed. Thus the BTF is

$$R(u) = f(u) + ig(u) = \frac{u+i}{u^2+1}\ . \tag{14.25}$$

which is equal to the Fourier transform of the SRF $G(t)$ multiplied by $-i/(4\pi\Delta\omega)$. These results are depicted in Fig. 14.2. As expected the shock excitation is the decay of the center displacement $\langle x\rangle$ or the center velocity displacement $\langle\dot{x}\rangle$. The decay comes from the distribution $\rho(\omega)$ so that each particle oscillates with a slightly different frequency. The particles will spread out and therefore the decay of the center displacement or the center velocity displacement. This is usually known as *decoherence* or *filamentation*. For the Lorentz distribution, the decay turns out to be exponential. However, it is important to point out that the center $\langle\dot{x}\rangle$ decays because initially we have a nonzero x_0 but $\dot{x}_0=0$. In case $\dot{x}_0\neq 0$, the Lorentz distribution *does not* gives a decay of the center displacement, (Exercise 14.1).

Table 13.4 lists the BTF and SRF for some commonly used frequency distributions (Exercise 14.2).

Because the BTF is the Fourier transform of SRF, $G(t)$ is also the inverse Fourier transform of $R(u)$:

$$G(t) = \mathcal{R}e\,\frac{-i}{4\pi\Delta\omega}\int_{-\infty}^{\infty} d\omega\, R\left(\frac{\omega_x-\omega}{\Delta\omega}\right)e^{-i\omega t}\ . \tag{14.26}$$

The $\mathcal{R}e$ should not be there. It is there because we have consistently neglected the frequencies around $-\omega_x$.

14.3 LANDAU DAMPING

After understanding the BTF and the SRF, let us come back to the transient response

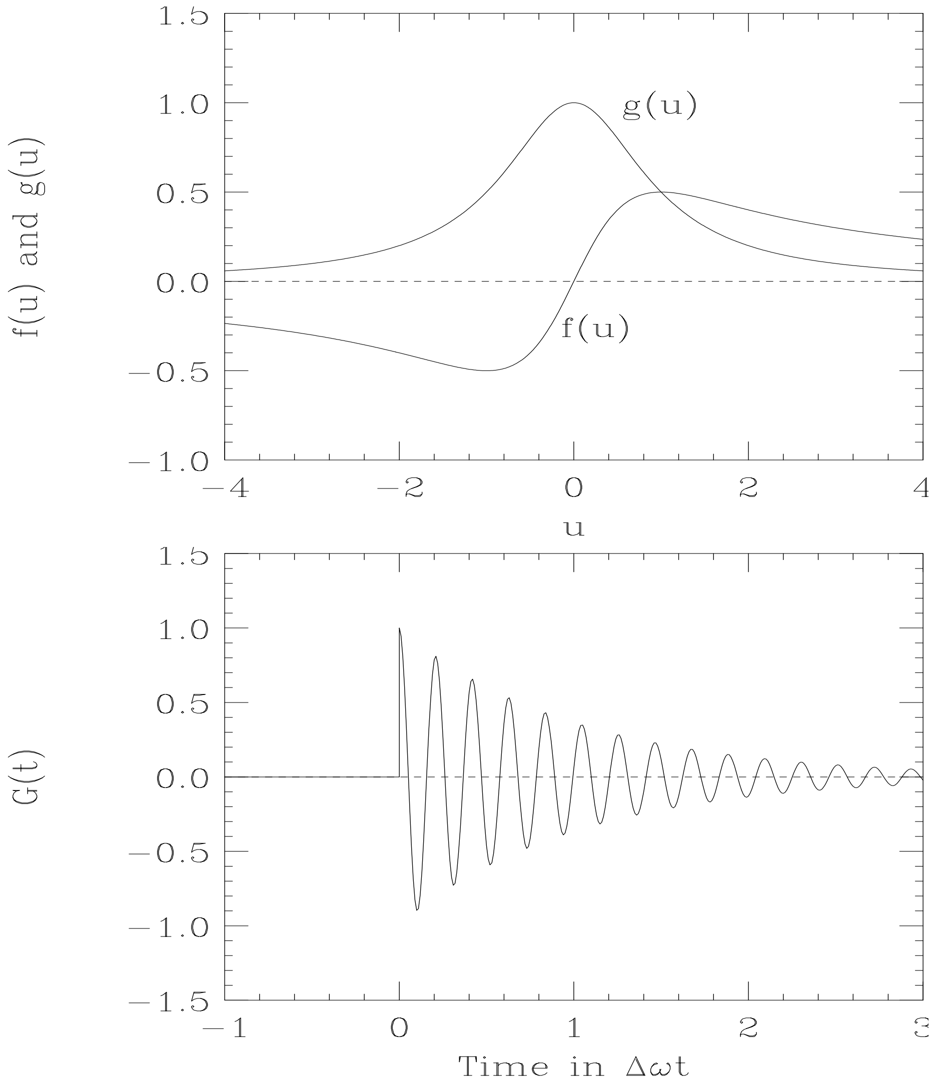

Figure 14.2: For Lorentz frequency distribution, plots showing beam transfer function $R(u) = f(u) + ig(u)$ (top) and shock response function $G(t)$ (bottom).

Figure 14.1: Shock excitation function $G(t)$ and beam transfer function $R(u) = f(u) + ig(u)$ for various frequency distributions $\rho(\omega)$ with $v = (\omega_x - \omega)/\Delta\omega$.

Frequency Distribution		Shock Response	Beam response function	
Type	Distribution	$G(t)$	$f(u)$	$g(u)$
Lorentz	$\frac{1}{\pi\Delta\omega}\frac{1}{v^2+1}$	$e^{-\Delta\omega\, t}\cos\omega_x t$	$\frac{u}{u^2+1}$	$\frac{1}{u^2+1}$
rectangular	$\frac{1}{2\Delta\omega}H(1-\lvert v\rvert)$		$\frac{1}{2}\ln\left\lvert\frac{u+1}{u-1}\right\rvert$	$\frac{\pi}{2}H(1-\lvert u\rvert)$
parabolic	$\frac{3}{4\Delta\omega}(1-v^2)H(1-\lvert v\rvert)$		$\frac{3}{4}\left[(1-u^2)\ln\left\lvert\frac{u+1}{u-1}\right\rvert+2u\right]$	$\frac{3\pi}{4}(1-u^2)H(1-\lvert v\rvert)$
elliptical	$\frac{2}{\pi\Delta\omega}\sqrt{1-v^2}H(1-\lvert v\rvert)$		$2\left[u-\mathrm{sgn}(u)\sqrt{1-u^2}H(1-\lvert u\rvert)\right]$	$2\sqrt{1-u^2}H(1-\lvert u\rvert)$
bi-Lorentz	$\frac{2}{\pi\Delta\omega}\frac{1}{(v^2+1)^2}$		$\frac{u(u^2+3)}{(u^2+1)^2}$	$\frac{2}{(u^2+1)^2}$
Gaussian	$\frac{1}{\sqrt{2\pi}\Delta\omega}e^{-v^2/2}$	$e^{-(\Delta\omega\, t)^2/2}\cos\omega_x t$	$\sqrt{\frac{2}{\pi}}e^{-u^2/2}\int_0^\infty\frac{dy}{y}e^{-y^2/2}\sinh\, uy$	$\sqrt{\frac{\pi}{2}}e^{-u^2/2}$

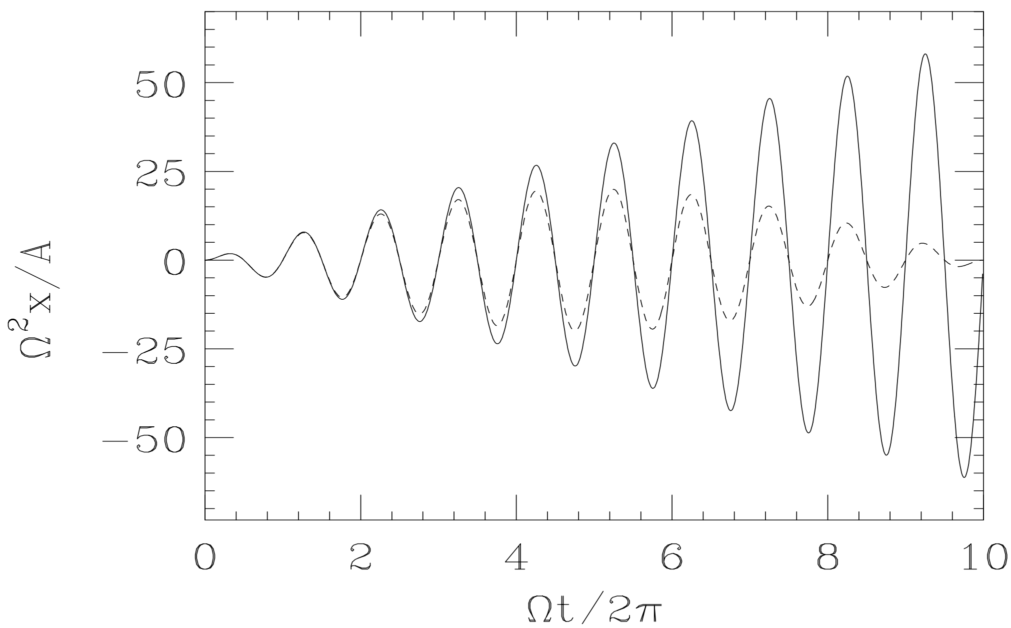

Figure 14.3: Solid: the response of a particle having exactly the same frequency Ω as the driving force grows linearly in time. Dashes: the response of a particle having frequency 95% of Ω gives up its energy after about 10 oscillations.

of a harmonic excitation; i.e., Eq. (14.4). The term proportional to $\sin\Omega t$ is driven in phase by the harmonic force, and the particle should be absorbing energy. Consider a component corresponding to the frequency ω, its envelope is, according to Eq. (14.3),

$$\text{Amplitude}(\omega) = \frac{A}{\omega_x}\,\frac{\sin(\omega-\Omega)t/2}{\omega-\Omega}\ . \tag{14.27}$$

This means that all particles that have frequency ω are excited at $t = 0$ increase to a maximum of $A/[\omega_x(\omega-\Omega)]$ at $t \approx \pi/(\omega-\Omega)$ and die down to zero again at $t = 2\pi/(\omega-\Omega)$. Thus energy is gained but is given back to the system. For ω closer to Ω, the response amplitude rises to a larger amplitude and the energy is given back to the system at a later time. For those particles that have exactly frequency Ω, the amplitude grows linearly with time and the energy keeps on growing. This is called *Landau damping*. An illustration is shown in Fig. 14.3, where the solid curve shows a particle having exactly the same frequency as Ω and growing linearly, while the dashed curve shows a particle with frequency 95% of Ω, decaying after about 10 oscillations. In other words, particles with ω far away from Ω get excited, but the energy is returned to those particles having ω close to Ω, which are still absorbing energy. As time increases, particles with frequencies closer to Ω give up their energies to particles with frequencies much closer to Ω. Thus, as time progresses, less and less particles are still absorbing energy. As $t \to \infty$, only particles with frequency exactly equal to Ω will be absorbing energy, and there are only very few particles doing this. So particles with frequencies very close to Ω will have their amplitudes keep on increasing. In practice, when these growing amplitudes hit the vacuum chamber, the process will stop. This sets the time limit for Landau damping to stop. The damping process starts when the amplitude of the first particle is damped and this time is $t \approx 2\pi/\Delta\omega$.

Let us study the energy in the system. The energy is proportional to the square of the amplitude. Therefore the energy of all the particles is

$$\mathcal{E} = \frac{NA^2}{\omega_x^2} \int_{-\infty}^{\infty} d\omega\, \rho(\omega)\, \frac{\sin^2(\omega-\Omega)t/2}{(\omega-\Omega)^2}\ , \tag{14.28}$$

where N is the total number of beam particles in the system. We see that as time progresses the amplitude square,

$$\text{Amplitude}(\omega)^2 = \frac{\sin^2(\omega-\Omega)t/2}{(\omega-\Omega)^2}\ , \tag{14.29}$$

becomes sharper and sharper while its width shrinks. This verifies that energy is being transfered by the particles having frequencies far away from Ω to particles having frequencies closer to Ω. Since the square of the amplitude always has an area of $\pi t/2$, we have

$$\lim_{t\to\infty} \text{Amplitude}(\omega)^2 = \lim_{t\to\infty} \frac{\sin^2(\omega-\Omega)t/2}{(\omega-\Omega)^2} = \frac{\pi t}{2}\,\delta(\omega-\Omega)\ . \tag{14.30}$$

Thus, at $t \to \infty$, the steady-state energy of the system is

$$\mathcal{E} = \frac{\pi}{2}\,\frac{NA^2}{\omega_x^2}\,\rho(\Omega)t\ , \tag{14.31}$$

which increases linearly with time, and all this energy goes into those few particles having exactly the same frequency as Ω. However, we do see in the asymptotic solution of Eq. (14.8) that $\langle x(t)\rangle$ does not go to infinity. This is not a contradiction, because even when a few particles have very large and still growing amplitudes, the centroid will not be affected.

In our study so far, the driving force has an amplitude A that is independent of the system of particles. For a particle beam, the situation is slightly different. The driving force comes from the wake fields of the beam particles interacting with the discontinuities of the vacuum chamber, and usually has an amplitude proportional to the center displacement of the beam. When there is a kick to the beam that creates a center displacement $\langle x(0)\rangle$ or a center displacement velocity $\langle \dot{x}(0)\rangle$, a force is generated and drives the whole system of particles. Now two things happen. First, the particles give up their excited energy to those particles having frequencies extremely close up Ω, the frequency of the driving force, and the center of displacement approaches the BTF $R(u)$. Second, the center of displacement of the beam starts to decay according to the SRF $G(t)$. As $\langle x(t)\rangle$ decreases, the driving force decreases also. Finally, the disturbance goes away. This is how Landau damping takes place in a bunch. In fact, this process starts whenever the disturbance is of infinitesimal magnitude. This implies that any disturbance will be damped as soon as it occurs. We say that there will be enough Landau damping to keep the beam stable. Notice that no frictional force has ever been introduced in the discussion. Thus, there is still conservation of energy in the presence of Landau damping, which merely redistributes energy from one wave to another.

14.4 TRANSVERSE BUNCH INSTABILITIES

Here, the frequency of the particle is the betatron frequency ω_β that has included the incoherent tune shift. The equation of motion is

$$\frac{d^2y}{ds^2} + \left(\frac{\omega_\beta}{\beta c}\right)^2 y = \frac{\langle F(\bar{y})\rangle}{\gamma m\beta^2c^2} , \tag{14.32}$$

coming from Eq. (2.4) in Chapter 2 where the dependence of the average force on y has been absorbed into ω_β. The force is related to the transverse wake function,

$$\langle F(\bar{y})\rangle = -\frac{e^2N}{C}\sum_{k=1}^{\infty}\bar{y}(s-kC)W_1(kC) \tag{14.33}$$

where the summation is over previous turns. The negative sign shows that the force is opposing the displacement. The absence of the linear particle density indicates that we are dealing with a point bunch. Here $\bar{y}$ is the same as $\langle y\rangle$, denoting the center-of-mass displacement. Essentially the bunch considered here contains N particles all having the same longitudinal position, but they have different transverse displacements and betatron frequencies. Let us denote a collective instability of the dipole moment of the bunch $e\bar{y}(s)$ at the collective frequency Ω by the ansatz

$$\bar{y}(s) = De^{-i\Omega s/(\beta c)} , \tag{14.34}$$

where $\Omega \to \Omega + i\epsilon$ is assumed. Expressing in terms of the transverse impedance $Z_1^\perp$, Eq. (14.32) becomes

$$\frac{d^2y}{ds^2} + \left(\frac{\omega_\beta}{\beta c}\right)^2 y = \frac{ie^2ND}{\gamma mcC^2}\sum_{p=-\infty}^{\infty} Z_1^\perp(\Omega + p\omega_0)e^{-\Omega s/(\beta c)} \ , \tag{14.35}$$

and

$$\begin{aligned}\bar{y}(s) &= \frac{ie^2ND\beta^2c\mathcal{Z}}{2\omega_{\beta x}\gamma mC^2}\, e^{-i\Omega s/(\beta c)} \int_{-\infty}^{\infty} d\omega \frac{\rho(\omega)}{\omega - \Omega - i\epsilon} \\ &= \frac{ie^2ND\beta^2c\mathcal{Z}}{2\omega_{\beta x}\Delta\omega\gamma mC^2}\, e^{-i\Omega s/(\beta c)} R(u) \ ,\end{aligned} \tag{14.36}$$

where the relation has been made to the BTF $R(u)$, $\omega_{\beta x}$ is the center frequency of the distribution $\rho(\omega)$ with a spread $\Delta\omega$, and we have introduced a short-hand form for the impedance

$$\mathcal{Z} = \sum_{p=-\infty}^{\infty} Z_1^\perp(\Omega + p\omega_0) \ . \tag{14.37}$$

Now the ansatz of Eq. (14.34) is employed for $\langle y(t)\rangle$, giving the dispersion relation

$$\frac{ie^2N\beta^2c\mathcal{Z}}{2\omega_\beta\Delta\omega\gamma mC^2} = \frac{1}{R(u)} \ , \tag{14.38}$$

where the subscript x in ω_β has been dropped for convenience. If we come back to Eq. (14.35) and assume all particles have the same betatron frequency, we obtain the coherent tune shift

$$(\Delta\omega_\beta)_{\rm coh} = -\frac{ie^2N\beta^2c\mathcal{Z}}{2\omega_\beta\gamma mC^2} \tag{14.39}$$

which is just the left side of Eq. (14.38). Notice that when $\mathcal{R}e\, Z_1^\perp(\omega) < 0$, the coherent tune shift has a positive imaginary part and the bunch will be unstable, which is the situation without Landau damping. Now, Eq. (14.38) can be written as

$$-\frac{(\Delta\omega_\beta)_{\rm coh}}{\Delta\omega} = \frac{1}{R(u)} \ . \tag{14.40}$$

The locus of real u in the complex $1/R(u)$ plane is the threshold curve, and is plotted in Fig. 14.4 for various distributions. Remember that instability is generated by $\Omega \to \Omega + i\epsilon$ with ϵ real and positive. This translates to $u \to u - i\epsilon$. For the Lorentz distribution, the unstable region is therefore at

$$\frac{1}{R(u - i\epsilon)} = u - i(1+\epsilon) \ , \tag{14.41}$$

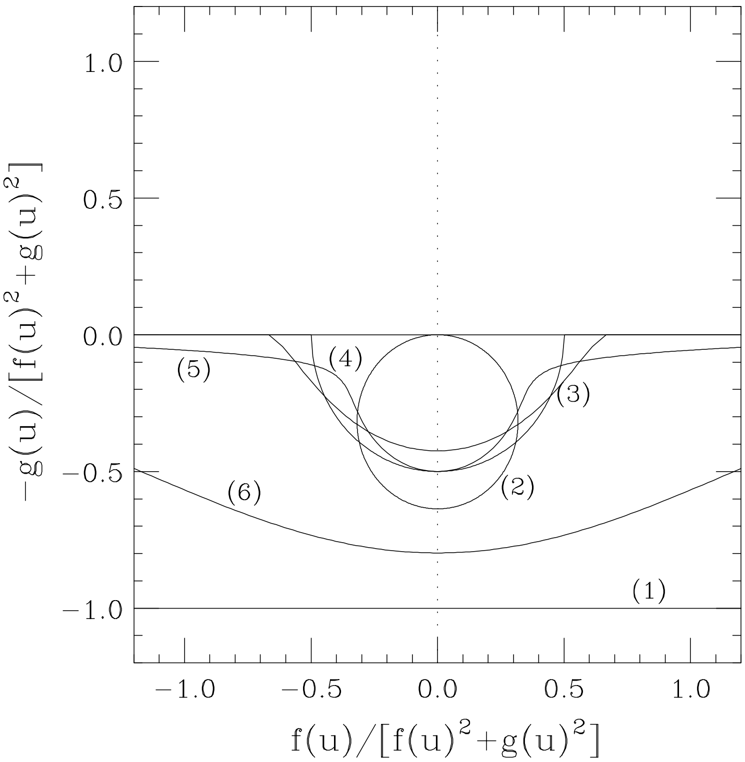

Figure 14.4: Threshold curves in the $1/R(u)$ plane, where in every case the stability region is to the top of the curve and the instability region to the bottom. (1) Lorentz distribution, (2) rectangular distribution (a circle touching the V-axis), (3) parabolic distribution, (4) elliptical distribution (part of the dashed circle centered at origin), (5) bi-Lorentz distribution, (6) Gaussian distribution.

while the stable region is above $\mathcal{I}m\, R(u)^{-1} = -1$. Since the various distributions have been introduced with all different definitions of frequency spread $\Delta\omega$, Fig. 14.4 is not a good plot for the comparison of various distributions. Instead, we would like to reference everything with respect to the HWHM frequency spread $\Delta\omega_{\text{HWHM}}$. Thus, we define a new variable x to replace u:

$$u = xS \qquad \text{with} \qquad S = \frac{\Delta\omega_{\text{HWHM}}}{\Delta\omega}\ . \tag{14.42}$$

The dispersion relation of Eq. (14.40) is rewritten as

$$-\frac{(\Delta\omega_\beta)_{\text{coh}}}{\Delta\omega_{\text{HWHM}}} = \frac{1}{\hat{R}(x)}\ . \tag{14.43}$$

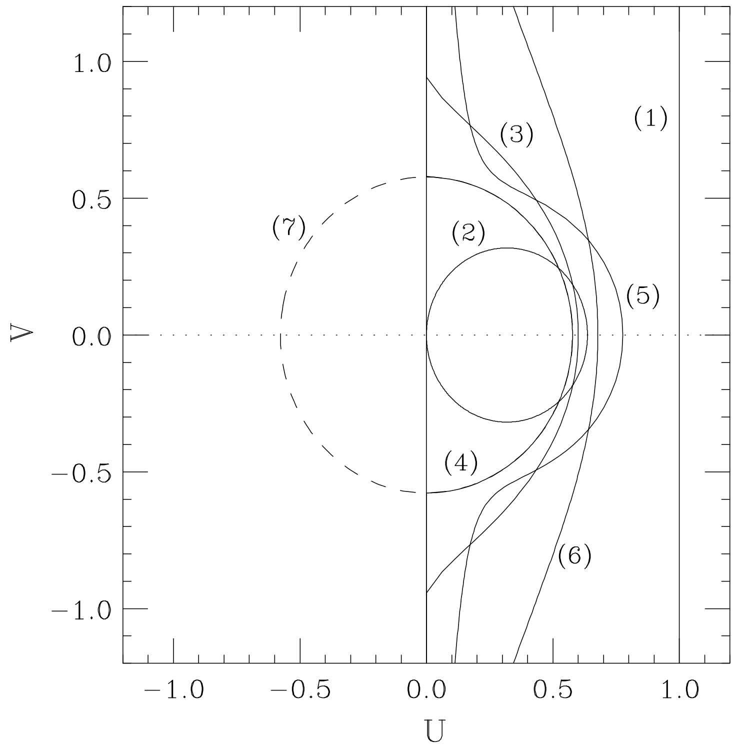

Figure 14.5: Threshold curves in the U-V plane plotted with reference to the HWHM frequency spread. In every case the stability region is to the left of the curve and the instability region to the right. (1) Lorentz distribution, (2) rectangular distribution (a circle touching the V-axis), (3) parabolic distribution, (4) elliptical distribution (part of the dashed circle centered at origin), (5) bi-Lorentz distribution, (6) Gaussian distribution. The Keil-Schnell type stability circle is depicted in dashes by (7).

where

$$\hat{R}(x) = \hat{f}(x) + i\hat{g}(x) = [f(u) + ig(u)]S \ . \tag{14.44}$$

It is customary to call the left side of Eq. (14.43) $i(U + iV)$, following the counterpart in longitudinal microwave threshold, or

$$U + iV = \frac{i}{\hat{R}(x)} = \frac{i\hat{f}(x) + \hat{g}(x)}{\hat{f}^2(x) + \hat{g}^2(x)} \ . \tag{14.45}$$

so that $U \propto -\mathcal{R}e\, Z_1^\perp$ and $U \propto -\mathcal{I}m\, Z_1^\perp$. The threshold curves for various frequency distributions are plotted in Fig. 14.5. Thus, whatever values of (U, V) lie to the left of the locus will be stable and whatever is on the right will be unstable. Without Landau damping, any $U > 0$, which implies betatron frequency shift with a positive imaginary part, will be unstable. Now, with Landau damping, the threshold has shifted to, for example, $U = 1$ for the Lorentz distribution. There is one point on the stability curve that is simple to obtain. It is the point at $x = 0$. There $\hat{f}(x) = 0$, so that $V = 0$ and $U = 1/\hat{g}(0)$. This point is important because it gives a rough idea of the threshold of instability. Similar to the Keil-Schnell stability circle for longitudinal microwave stability, we try to enclose the stability region in the U-V plane by a circle of radius $\frac{1}{\sqrt{3}}$, which is shown in Fig. 14.5 as a dashed circle. This threshold circle coincides with the semi-circle of the elliptical distribution. Thus, the stability limit can be written as

$$\left|(\Delta\omega_\beta)_{\rm coh}\right| \lesssim \frac{1}{\sqrt{3}}(\Delta\omega_\beta)_{\rm HWHM}F \ , \tag{14.46}$$

F is a form factor depending on the distribution and is equal to unity for the elliptical distribution. These are tabulated in Table 14.2 for various distributions (Exercise 14.3). Figure 14.5 shows how far a frequency distribution has its instability threshold deviated from the Keil-Schnell type circle of Eq. (14.46). We see that the deviation increases as the distribution goes from elliptical, parabolic, rectangular, Gaussian, bi-Lorentz, to Lorentz.

Thus, a betatron tune spread can provide Landau damping for instabilities driven by the discontinuities of the vacuum chamber, provided that the driving impedance is not too large. The transverse mode-mixing of mode-coupling instabilities that we studied in Chapter 12 have not had Landau damping included. However, mode-coupling instability involves the coherent shifting of a betatron spectral line by as much as the synchrotron frequency. In order for Landau damping to work, a betatron tune spread of the order of the synchrotron frequency will be necessary. This will be quite simple for proton machines where the synchrotron tune is of the order $\nu_s \sim 0.001$. This explains why transverse mode-mixing instabilities are usually not seen in proton machines. On the other hand, the synchrotron tunes for electron machines are usually $\nu_s \sim 0.01$. A betatron tune spread of this size will be too large. For this reason, transverse mode-mixing instabilities in electron machines are usually alleviated by reactive dampers.

14.5 LONGITUDINAL BUNCH INSTABILITIES

In a bunch, Landau damping proceeds through the spread in synchrotron frequency. Again let us consider a point bunch whose longitudinal displacement at position s is

Table 14.2: U-intercept and form factor F defined in Eq. (14.46) for various distributions.

Distribution	$g(0)^{-1}$	$S = \dfrac{(\Delta\omega_\beta)_{\text{HWHM}}}{\Delta\omega}$	U-intercept $\hat{g}(0)^{-1} = g(0)^{-1} S^{-1}$	Form factor $F = \sqrt{3}\hat{g}(0)^{-1}$
Lorentz	1	1	1	$\sqrt{3}$
rectangular	$\dfrac{2}{\pi}$	1	$\dfrac{2}{\pi}$	$\dfrac{2\sqrt{3}}{\pi}$
parabolic	$\dfrac{4}{3\pi}$	$\dfrac{1}{\sqrt{2}}$	$\dfrac{4\sqrt{2}}{3\pi}$	$\dfrac{4}{\pi}\sqrt{\dfrac{2}{3}}$
elliptical	$\dfrac{1}{2}$	$\dfrac{\sqrt{3}}{2}$	$\dfrac{1}{\sqrt{3}}$	1
bi-Lorentz	$\dfrac{1}{2}$	$\sqrt{\sqrt{2}-1}$	$\dfrac{1}{2\sqrt{\sqrt{2}-1}}$	$\dfrac{1}{2}\sqrt{\dfrac{3}{\sqrt{2}-1}}$
Gaussian	$\sqrt{\dfrac{2}{\pi}}$	$\sqrt{2\ln 2}$	$\dfrac{1}{\sqrt{\pi\ln 2}}$	$\sqrt{\dfrac{3}{\pi\ln 2}}$

described by $z(s)$. The equation of motion is

$$\begin{aligned}\frac{d^2z}{ds^2} + \left(\frac{\omega_s}{\beta c}\right)^2 z &= \frac{e^2N\eta}{\beta EC}\sum_{k=1}^{\infty} W_0'\Big(kC + \langle z(s-kC)\rangle - \langle z(s)\rangle\Big) \\ &\approx \frac{e^2N\eta}{\beta EC}\Big(\langle z(s-kC)\rangle - \langle z(s)\rangle\Big)\sum_{k=-\infty}^{\infty} W_0''(kC)\ , \end{aligned} \tag{14.47}$$

where E is the particle energy, and the term corresponding to potential-well distortion has not been included in the last line. This can be written as

$$\frac{d^2z}{ds^2} + \left(\frac{\omega_s}{\beta c}\right)^2 z = -\frac{ie^2N\eta B\omega_0\mathcal{Z}_\parallel}{\beta EC^2}\ , \tag{14.48}$$

where we have used the ansatz

$$\langle z(s)\rangle = Be^{-i\Omega s/(\beta c)}\ , \tag{14.49}$$

and the short-hand notation

$$\mathcal{Z}_\parallel = \sum_{p=-\infty}^{\infty} \left[\left(p + \frac{\Omega}{\omega_0} \right) Z_0^\parallel(p\omega_0 + \Omega) - p Z_0^\parallel(p\omega_0) \right] . \tag{14.50}$$

Now solve for $z(s)$ and integrate with the distribution of synchrotron frequency $\rho(\omega_s)$. Then, self-consistency leads to the dispersion relation

$$-\frac{ie^2 N\omega_0 v^2 \eta \mathcal{Z}_\parallel}{2\omega_s \beta E C^2 \Delta\omega} = \frac{1}{R(u)} . \tag{14.51}$$

Without any spread in the synchrotron frequency, we obtain the coherent synchrotron frequency shift

$$(\Delta\omega_s)_{\rm coh} = \Omega - \omega_s = \frac{ie^2 N\omega_0 v^2 \eta \mathcal{Z}_\parallel}{2\omega_s \beta E C^2} . \tag{14.52}$$

If the narrow resonance impedance has its resonant frequency ω_r detuned to below the rf frequency,

$$\mathcal{R}e\, \mathcal{Z}_\parallel \approx \frac{\omega_r}{\omega_0} \left[\mathcal{R}e\, Z_0^\parallel(\Omega + p\omega_0) - \mathcal{R}e\, Z_0^\parallel(\Omega - p\omega_0) \right] < 0 , \tag{14.53}$$

where $\Omega \approx \omega_s$. Above transition ($\eta > 0$), this leads to stability in agreement with Robinson stability criterion. Thus, from Eq. (14.51), we can again write

$$-\frac{(\Delta\omega_s)_{\rm coh}}{\Delta\omega} = \frac{1}{R(u)} . \tag{14.54}$$

Therefore, we can define

$$U + iV = -i\frac{(\Delta\omega_s)_{\rm coh}}{\Delta\omega} = \frac{i}{R(u)} = \frac{g(u) + if(u)}{f^2(u) + g^2(u)} . \tag{14.55}$$

The stability threshold curve in the U-V plane will therefore be exactly the same as in the transverse bunch instability analyzed in the previous section. The Keil-Schnell like stability circle is

$$(\Delta\omega_s)_{\rm coh} \lesssim \frac{1}{\sqrt{3}} (\Delta\omega_s)_{\rm HWHM} F , \tag{14.56}$$

where $(\Delta\omega_s)_{\rm HWHM}$ is the half-width-at-half-maximum of the synchrotron frequency spread, and the form factors F for various distribution are exactly the same as given in Table 14.2.

The above example is a demonstration of Landau damping in the presence of Robinson stability or instability. Therefore, even if the rf resonant peak is shifted in the wrong way so that we have Robinson instability, there is still Landau damping due to the spread in synchrotron frequency.

14.6 TRANSVERSE UNBUNCHED BEAM

Consider a particle in the unbunched beam. Its transverse displacement $y(s,t)$ satisfies the equation

$$\frac{d^2y}{dt^2}+\omega_\beta^2 y=\frac{\langle F(s,t)\rangle}{\gamma m}\ , \tag{14.57}$$

where the particle is at location s along the ring at time t. For an unbunched beam, the revolution harmonic should be a good eigen-number. Consider the perturbing part of the beam distribution, which contributes a dipole moment D per unit length, where

$$D(s,t)=\frac{eN}{C}\langle y(s,t)\rangle=\frac{eN\Delta}{C}\exp\left(in\frac{s}{R}-i\Omega t\right)\ . \tag{14.58}$$

The average transverse force is

$$\begin{aligned}\langle F(s,t)\rangle &= -\frac{e}{C}\int_{-\infty}^{\infty} v dt' W_1(vt-vt')D(s,t') \\ &= \frac{iev\beta D(s,t)Z_1^\perp(\Omega)}{C}\ .\end{aligned} \tag{14.59}$$

Here, s and t are related by $s=S+ct$ where S is the position of the particle at time $t=0$. Then the equation of motion becomes

$$\ddot{y}+\omega_\beta^2 y=\frac{ie^2N\beta^2cZ_1^\perp(\Omega)\Delta}{\gamma mC^2}\exp\left[in\frac{S}{R}-i(\Omega-n\omega_0)t\right]\ , \tag{14.60}$$

which can now be integrated to give

$$y(s,t)=\frac{ie^2N\beta^2cZ_1^\perp(\Omega)\Delta}{\gamma mC^2}\frac{e^{ins/R-i\Omega t}}{\omega_\beta^2-(\Omega-n\omega_0)^2}\ . \tag{14.61}$$

Integrating with the betatron frequency distribution $\rho(\omega)$ gives the self-consistent dispersion relation

$$1=\frac{ie^2N\beta^2cZ_1^\perp(\Omega)}{\gamma mC^2}\int d\omega\,\frac{\rho(\omega)}{\omega^2-(\Omega-n\omega_0)^2}\approx-(\Delta\omega_\beta)_{\rm coh}\int d\omega\,\frac{\rho(\omega)}{\omega-(\Omega-n\omega_0)}\ , \tag{14.62}$$

where

$$(\Delta\omega_\beta)_{\rm coh} = \Omega - n\omega_0 - \omega_\beta = -\frac{ie^2N\beta^2cZ_1^\perp(\Omega)}{2\omega_\beta\gamma mC^2} \tag{14.63}$$

is the coherent betatron frequency shift. Thus, again we have

$$-\frac{(\Delta\omega_\beta)_{\rm coh}}{\Delta\omega} = \frac{1}{R(u)} \ . \tag{14.64}$$

exactly the same as Eq. (14.40). The only difference is the dependence of the coherent betatron tune shift on impedance is different. Thus, we have also the Keil-Schnell like stability threshold

$$(\Delta\omega_\beta)_{\rm coh} \lesssim \frac{1}{\sqrt{3}}(\Delta\omega_\beta)_{\rm HWHM}F \ . \tag{14.65}$$

14.7 LONGITUDINAL UNBUNCHED BEAM

This instability is different from what we have discussed before, because we have no synchrotron frequency here. Landau damping is supplied by the spread in revolution frequency of the beam particles. This is the longitudinal microwave instability. The dispersion relation, Eq. (5.12), has been derived in Chapter 5 and the stability curves are shown in Fig. 5.4. Formerly, the dispersion relation was derived using Vlasov equation. Here, we will show another derivation without resorting to Vlasov equation.

The phase space distribution is

$$\psi(s,t,\omega_0) = \big[\lambda_0 + \Delta\lambda(s,t)\big]\rho(\omega_0) \ , \tag{14.66}$$

where $\rho(\omega_0)$ is the distribution in revolution frequency, and the unperturbed linear density is just

$$\lambda_0 = \frac{N}{C} \ . \tag{14.67}$$

The average longitudinal force depends only on the linear distribution and is given by

$$\begin{aligned} \langle F(s,t)\rangle \ &= \ -\frac{e^2}{C}\int vdt'W_0'(vt-vt')\Delta\lambda(s,t') \\ &= \ -\frac{e^2vZ_0^\parallel(\Omega)}{C}\Delta\lambda(s,t) \ , \end{aligned} \tag{14.68}$$

where the ansatz

$$\Delta\lambda(s,t) = \widehat{\Delta\lambda}e^{ins/R-i\Omega t} \tag{14.69}$$

has been used.

A particle will drift by $z(s,t)$ longitudinally according to

$$\dot{z} = -\eta v \delta \ , \tag{14.70}$$

while the rate of change of the fractional momentum spread δ is

$$\dot{\delta} = -\frac{e^2c^2}{CE} Z_0^{\|}(\Omega)\Delta\lambda(s,t) \tag{14.71}$$

This particle is at location S at time $t=0$, or $s = S + vt$. Thus

$$\dot{\delta} = -\frac{e^2c^2}{CE} Z_0^{\|}(\Omega)\widehat{\Delta\lambda} e^{inS/R - i(\Omega - n\omega_0)t} \ . \tag{14.72}$$

Integration gives

$$\delta(t) = \frac{e^2c^2}{CE} Z_0^{\|}(\Omega)\widehat{\Delta\lambda} \frac{e^{inS/R - i(\Omega - n\omega_0)t}}{i(\Omega - n\omega_0)} \ , \tag{14.73}$$

$$z(t) = -\frac{e^2\eta c^2 v}{CE} Z_0^{\|}(\Omega) \frac{\Delta\lambda}{(\Omega - n\omega_0)^2} \ . \tag{14.74}$$

The particles that are originally at $\lambda_0 ds$ now move to a new volume. Therefore

$$\lambda_0 ds = \big[\lambda_0 + \Delta\lambda(s,t)\big]\Big\{\big[s + \Delta s + z_{s+\Delta s - vt}(t)\big] - \big[s + z_{s-vt}(t)\big]\Big\} \ . \tag{14.75}$$

This leads to the perturbed phase-space distribution

$$\begin{aligned} \Delta\lambda(s,t)\rho(\omega_0) &= -\lambda_0 \frac{\partial z}{\partial s}\bigg|_{s-vt} \rho(\omega_0) \\ &= \frac{ine^2 N\eta c^3 \beta Z_0^{\|}(\Omega)}{RC^2E} \frac{\Delta\lambda\rho(\omega_0)}{(\Omega - n\omega_0)^2} \ . \end{aligned} \tag{14.76}$$

Integrating both sides, consistency leads to the dispersion relation

$$1 = \frac{ine^2 N\eta c^3 \beta Z_0^{\|}(\Omega)}{RC^2E} \int d\omega_0 \frac{\rho(\omega_0)}{(\Omega - n\omega_0 + i\epsilon)^2} \ . \tag{14.77}$$

Define the growth rate without damping ω_L which is very similar to the synchrotron frequency:

$$\omega_L^2 = \frac{ieI_0 Z_0^{\|}(\Omega) n\eta\omega_0^2}{2\pi\beta^2 E} \ . \tag{14.78}$$

The dispersion relation can be rewritten as

$$1=\left[\frac{\omega_L^2}{n^2(\Delta\omega)^2}\right]\left[n(\Delta\omega)^2\int d\omega_0\frac{\rho'(\omega_0)}{n\omega_0-\Omega-i\epsilon}\right]=\left[\frac{\omega_L^2}{n^2(\Delta\omega)^2}\right]R_\parallel(u)\ , \tag{14.79}$$

where an integration by part has been performed. The function $R_\parallel$ on the right is defined as

$$R_\parallel(u)=f_\parallel(u)+ig_\parallel(u)=n(\Delta\omega)^2\,\wp\!\int d\omega_0\frac{\rho'(\omega_0)}{n\omega_0-\Omega}+i(\Delta\omega)^2\pi\rho'\left(\frac{\Omega}{n}\right)\ , \tag{14.80}$$

and

$$u=\frac{\omega_{0x}-\omega_0}{\Delta\omega}\ , \tag{14.81}$$

with $\Delta\omega$ a measure of the spread of the revolution frequency distribution $\rho(\omega_0)$ and ω_{0x} the center revolution frequency. Usually one writes

$$V-iU=\frac{\omega_L^2}{n^2(\Delta\omega)^2}=\frac{f_\parallel(u)-ig_\parallel(u)}{f_\parallel^2(u)+g_\parallel^2(u)}\ . \tag{14.82}$$

This will give the threshold and growth curves for longitudinal microwave instability in Chapter 5.

14.8 MORE ON BTF

Consider a coasting beam. In addition to the transverse wake, if we give an extra sinusoidal kick with harmonic n and frequency Ω, the equation of motion is

$$\ddot{y}+\omega_\beta^2y=-2(\Delta\omega_\beta)_{\rm coh}\omega_\beta\langle y\rangle+Ae^{ins/R-i\Omega t}\ , \tag{14.83}$$

where the coherent betatron tune shift $(\Delta\omega_\beta)_{\rm coh}$ is given by Eq. (14.39). For the particular solution, try the ansatz

$$\langle y(s,t)\rangle=Be^{ins/R-i\Omega t}\ . \tag{14.84}$$

As before, $s=S+vt$, and we obtain

$$y(s,t)=\frac{\big[-2(\Delta\omega_\beta)_{\rm coh}\omega_\beta B+A\big]e^{ins/R-i\Omega t}}{\omega_\beta^2-(n\omega_0-\Omega)^2}\ . \tag{14.85}$$

Consistency requires

$$B\approx\frac{-2(\Delta\omega_\beta)_{\rm coh}\omega_\beta B+A}{2\omega_\beta}\int d\omega\,\frac{\rho(\omega)}{\omega-(\Omega-n\omega_0)}=\frac{-2(\Delta\omega_\beta)_{\rm coh}\omega_\beta B+A}{2\omega_\beta\Delta\omega}R(u)\ , \tag{14.86}$$

and after rearranging,

$$\frac{A}{2\omega_\beta \Delta\omega B} = \frac{1}{R(u)} + \frac{(\Delta\omega_\beta)_{\mathrm{coh}}}{\Delta\omega} \ . \tag{14.87}$$

In a measurement, the beam is kicked at a certain harmonic but with various frequencies ω and the response is measured in its amplitude and phase. If the beam is of very weak intensity, the coherent tune shift term can be neglected and one can therefore obtain the BTF $R(u)$. Next, the beam intensity is increased to such a large value that the beam is still stable. The measurement of the beam response will give a stability curve shifted by $(\Delta\omega_\beta)_{\mathrm{coh}}/\Delta\omega$. From the shift one can therefore infer the impedance $Z_1^\perp$ of the vacuum chamber as illustrated in the top plot of Fig. 14.6

For the longitudinal BTF, we add a longitudinal kicking voltage per unit length, A with revolution harmonic n and frequency Ω. Then the longitudinal force seen by a particle changes from Eq. (14.68) to

$$\langle F(s,t)\rangle = -\frac{e^2}{C}\int v dt' W_0'(vt-vt')\Delta\lambda(s,t)\rho(\omega_0) + Ae^{ins/R-i\Omega t} \ . \tag{14.88}$$

Assume the ansatz

$$\Delta\lambda(s,t) = Be^{ins/R-i\Omega t} \ . \tag{14.89}$$

Then the solution of the momentum spread and longitudinal drift become

$$\delta(t) = \frac{\dfrac{-e^2c^2}{CE}Z_0^\parallel(\Omega)B + A}{-i(\Omega - n\omega_0)}\, e^{inS/R-i(\Omega-n\omega_0 t} \ . \tag{14.90}$$

$$z(t) = \eta v\frac{\dfrac{-e^2c^2}{CE}Z_0^\parallel(\Omega)B + A}{(\Omega - n\omega_0)^2}\, e^{ins/R-i\Omega t} \ . \tag{14.91}$$

Doing the same as Eqs. (14.76) and (14.77), we obtain

$$B = \left[\frac{\omega_L^2}{n^2(\Delta\omega)^2}B + \frac{i2\pi\eta vN}{n^2(\Delta\omega)^2C^2}A\right]R_\parallel(u) \ . \tag{14.92}$$

Or,

$$\frac{i2\pi\eta vN}{n^2(\Delta\omega)^2C^2}\,\frac{A}{B} = \frac{1}{R_\parallel(u)} - \frac{\omega_L^2}{n^2(\Delta\omega)^2} \ . \tag{14.93}$$

Exactly in the same way as the transverse counterpart, for a very low intensity beam, the response of the kick gives the threshold curve. For an intense beam, this threshold curve

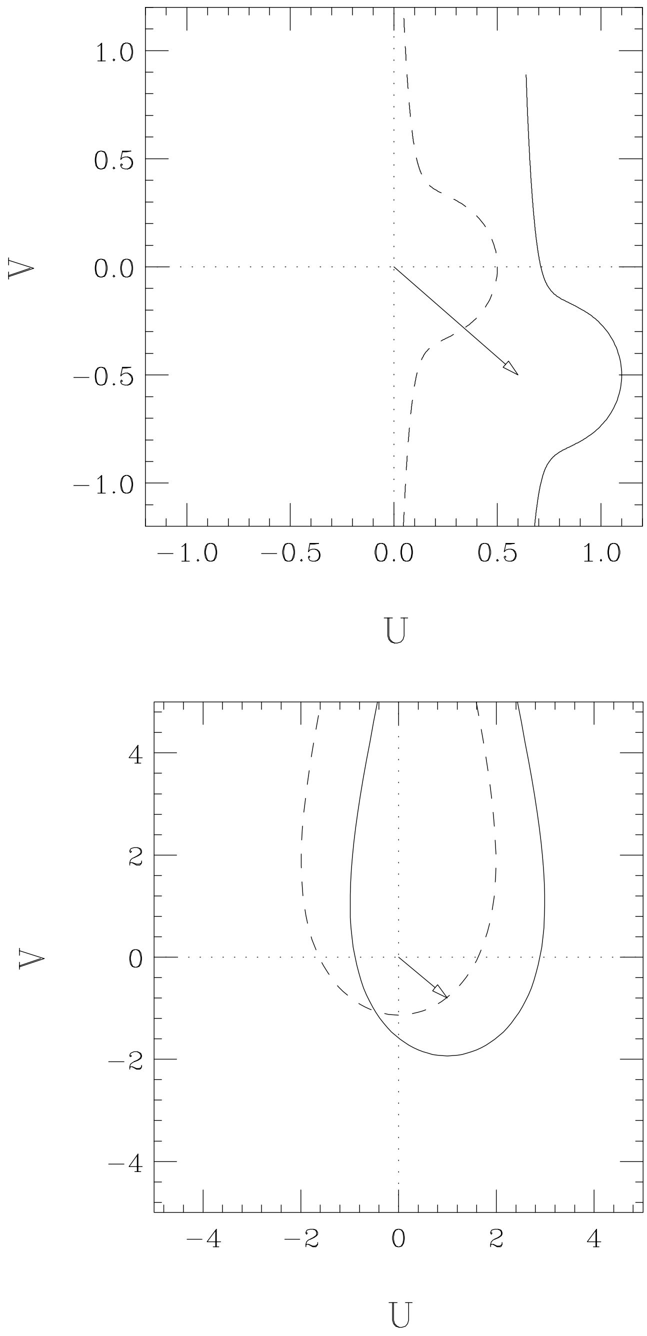

Figure 14.6: Top: Transverse beam response function of a coasting beam. Dash curve is for a very low intensity beam, thus showing the threshold curve. But it is shifted to the solid curve at high intensity. The transverse impedance can be inferred from the shift indicated by the arrow. Bottom: Longitudinal beam response function of a coasting beam. The dashed curve is for low intensity and is shifted to the solid curve at high intensity. The arrow is proportional to the longitudinal impedance.

will be shifted. The amount and direction of shift will be proportional to the magnitude and phase of the longitudinal impedance. This is shown in the lower plot of Fig. 14.6.

14.9 EXERCISES

14.1. A shock excitation is given to bunch with a Lorentz frequency distribution $\rho(\omega)$ so that at $t = 0$ each particle has $\dot{x}(t) = \dot{x}_0$. Compute the response of the displacement of the center of a bunch $\langle x(t) \rangle$ and show that it does not decay to zero. Show that this is because $\rho(0) \neq 0$.

14.2. Derive the shock response function $G(t)$ and beam transfer function $R(u)$ for the various frequency distributions as listed in Table 14.1. Fill in those items that have been left blank.

14.3. Derive the U-intercept and the form factor F defined in Eq. (14.46) for various distributions as listed in Table 14.2.

Bibliography

[1] L.D. Landau, J. Phys. USSR **10**, 25 (1946).

[2] J.D. Jackson, Nuclear Energy Part C: Plasma physics **1**, 171 (1960).

[3] V.K. Neil and A.M. Sessler, Rev. Sci. Instr. **6**, 429 (1965).

[4] L.J.Laslett, V.K. Neil, and A.M. Sessler, Rev. Sci. Instr. **6**, 46 (1965).

[5] H.G. Hereward, CERN Report 65-20 (1965).

[6] A. Hofmann, *Frontiers of Part. Beams: Intensity Limitations*, Hilton Head Island, Lecture in Phys. **400**, Springer-Verlag, 1990, p.110.

[7] A.W. Chao, *Physics of Collective Beam Instabilities in High Energy Accelerators*, Wiley Interscience, 1993, Chapter 5.